Dynamic Heterogeneities in Supercooled Water†

Nicolas Giovambattista,*,‡ Marco G. Mazza,‡ Sergey V. Buldyrev,‡ Francis W. Starr,§ and H. Eugene Stanley‡

Center for Polymer Studies and Department of Physics, Boston University, Boston, Massachusetts 02215, and Department of Physics, Wesleyan University, Middletown, Connecticut 06459

Received: December 18, 2003; In Final Form: February 6, 2004

We investigate dynamic heterogeneities in liquid water by performing molecular dynamics simulations of the SPC/E model. We find clusters of mobile molecules. We study the temperature and time dependence of the cluster size and find that clusters grow as temperature decreases and have a maximum size at the time scale corresponding to the escape of the molecules from the cage formed by neighboring molecules. We relate the average mass n^* of mobile particle clusters to the diffusion constant, D, and the configurational entropy, S_{conf}. We find that n^* can be interpreted as the mass of the "cooperatively rearranging regions" hypothesized in the Adam−Gibbs theory of the dynamics of supercooled liquids. In the context of the potential energy landscape (PEL) approach, the diffusion of molecules is related to the change of basins. By studying the dynamics of the system on the PEL, we identify clusters formed by the molecules with large displacements as the system visits consecutive local minima on the PEL. We relate the changing of basins with the restructuring of the hydrogen bond network.

I. Introduction

Supercooled liquids are characterized by the nonexponential decay of ensemble-averaged time correlation functions.[1−9] Two microscopic scenarios have been proposed to explain this behavior, schematically shown in Figure 1. In the spatially homogeneous dynamics scenario, correlation functions for different molecules decay in the same way, i.e., by a stretched exponential function $\exp[-(t/t_r)^{\beta}]$ with a characteristic relaxation time t_r and exponent β. As shown in Figure 1, in the "homogeneous" scenario, all molecules are equivalent. As the temperature is lowered, the locally averaged molecular displacement is the same at every point in the system. The homogeneous scenario is inconsistent with experiments[10−15] and simulations,[16−19] which identify dynamical heterogeneities in supercooled liquids and spin glasses.[20]

In the spatially heterogeneous dynamics (SHD) scenario, correlation functions for different molecules decay exponentially, but with a very broad distribution of relaxation times.[21] The superposition of these individual exponential contributions produces a nonexponential decay of the ensemble-averaged time correlation function, and the exponent β is a measure of the width of the distribution of relaxation times. In the heterogeneous scenario, the locally averaged molecular displacements are different depending on the part of the system we are looking at and when we look at it. One finds groups of molecules that are more mobile and groups that are less mobile than the average molecule in the system. As the temperature is lowered, patches formed by mobile molecules increase in size. These patches of mobile molecules have a short lifetime; they appear and disappear constantly in different parts of the system. In section II, we show that the SHD scenario describes the dynamics of supercooled water.

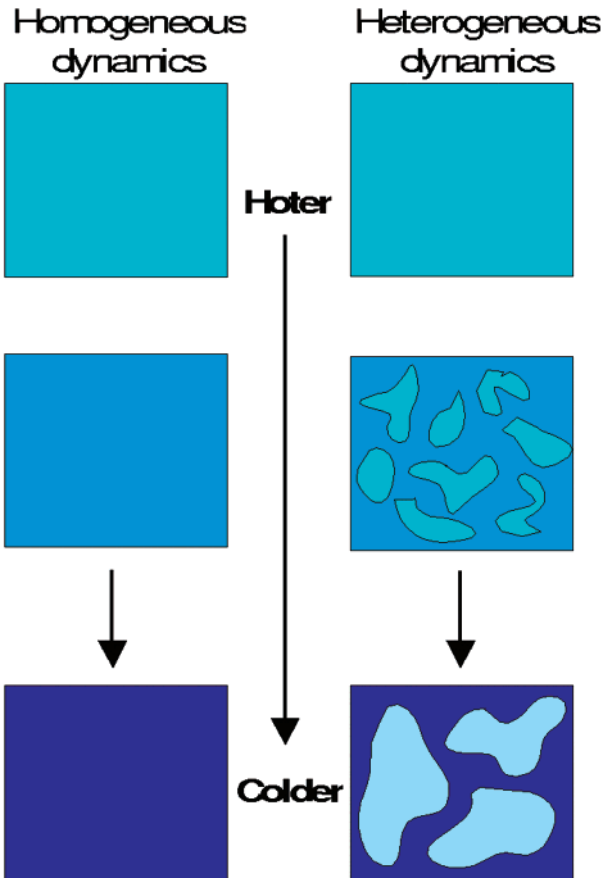

Figure 1. Two possible scenarios proposed to describe diffusion in cold liquids. In the spatially homogeneous dynamics scenario molecules relax in the same way, while in the spatially heterogeneous dynamics (SHD) scenario, sets of more mobile molecules (in comparison to the average motion of the molecules in the system) form patches or clusters. The size of these clusters increases upon cooling.

† Part of the special issue "Hans C. Andersen Festschrift".
* To whom correspondence should be addressed.
‡ Boston University.
§ Wesleyan University.

10.1021/jp037925w CCC: $27.50
Published on Web 04/13/2004

The potential energy landscape (PEL) formalism provides a theoretical approach to the study of supercooled liquids. The PEL for a system composed of N particles is the potential energy surface of a system in a (3N+1)-dimensional space. The system in this high-dimensional space is represented by a point. The diffusion of the particles in the system corresponds to the motion of the representative point of the system on the PEL.[1,2,22−25] As the liquid is cooled toward the glassy state, the ability of the particles to diffuse decreases and the system is increasingly found near local potential energy minima on the PEL, called inherent structure (IS) configurations.[23] A general picture has evolved[26−29] of the system moving among a set of basins, each corresponding to a local minimum. In the glassy state, when diffusion stops, the system is localized in one of the potential energy basins.

The number of basins available to the system has been related to the configurational entropy S_{conf}. The concept of configurational entropy was first introduced by Adam−Gibbs (AG).[30] The AG predictions were confirmed in computer simulations using the SPC/E model[31] and in other models of simple liquids.[32,33,34] However, the AG theory is based on the concept of cooperatively rearranging regions (CRR), which are not precisely defined. In section III, we relate the clusters formed by mobile molecules found in simulations[35] with the CRR from AG theory.

The PEL approach proposes that diffusion occurs by IS transitions, i.e., by moving from one basin to another. Furthermore, these IS transitions involve more subtle heterogeneities corresponding to rearrangement of localized set of molecules.[24] In section IV, we identify these more subtle heterogeneities associated to the IS transitions and relate them to the restructuring of the hydrogen-bond network. Finally, in section V, we discuss our results.

II. Spatially Heterogeneous Dynamics

Clusters composed of particles with high mobility have been found in numerical simulations of simple systems, e.g., Lennard-Jones (LJ) mixtures, indicating the presence of SHD.[10,16,19,36−44] Hence, the SHD scenario for the dynamics of liquids at low temperatures was confirmed in these systems. In this section, we show that SHD is also present in computer simulations of the SPC/E[45] water model as expected from previous findings for the ST2 and TIP4P models for water.[46,47] We study a system with $N = 1728$ molecules at fixed density $\rho = 1.0$ g/cm^3 varying the temperature T from 200 to 260 K in steps of 10 K. To increase statistics, we performed two independent simulations for every temperature. We find that the T dependence of the diffusion constant can be expressed by

$$D \sim (T - T_{MCT})^{\gamma} \tag{1}$$

where the mode coupling temperature $T_{MCT} = 193$ K and the diffusivity exponent $\gamma = 2.80$.[48,49]

We use the approach introduced in a study of a LJ mixture[37] to define mobile molecule clusters. We calculate the self-part of the time-dependent van Hove correlation function[50] $G_s(r, t)$

$$G_s(r, t) \equiv \frac{1}{N}\sum_{i=1}^{N}\langle \delta(|\vec{r}_i(t) - \vec{r}_i(0)| - r)\rangle \tag{2}$$

where $\langle\cdots\rangle$ represents an average over configurations and $\vec{r}_i(t)$ are the coordinates of the oxygen atom of the ith molecule. The probability of finding an oxygen atom at a distance r at time t from its position at $t = 0$ is given by $4\pi r^2 G_s(r, t)\, dr$.

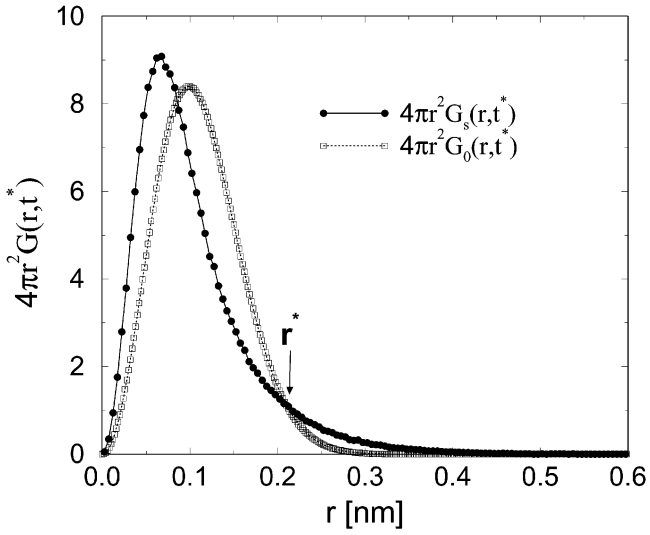

Figure 2. Van Hove correlation function $G_s(r, t^*)$ and its Gaussian approximation $G_0(r, t^*)$ obtained using $\langle r^2(t^*)\rangle$, for $T = 220$ K. The tails of the distributions cross at $r^* \approx 0.225$ for all temperature. In this work, we focus on the fraction ϕ of molecules with large displacements over an observation time Δt. ϕ is the probability that a molecule has a displacement $r \geq r^*$ in a time interval equal to t^* (area under the curve $4\pi r^2 G_s(r, t^*)$ for $r \geq r^*$).

For both short times (when particles move ballistically) and long times (when particle motion can be described by the diffusion equation), $G_s(r, t)$ can be fitted by a Gaussian approximation

$$G_0(r, t) = \left[\frac{3}{2\pi\langle r^2(t)\rangle}\right]^{3/2} \exp[-3r^2/2\langle r^2(t)\rangle] \tag{3}$$

where $\langle r^2(t)\rangle$ is the mean square displacements of the oxygen atoms. However, deviations of $G_s(r, t)$ from $G_0(r, t)$ are well pronounced at intermediate times, corresponding to the vibrations of the particles within the cage formed by neighboring molecules. We define t^* as the value of time at which the deviation of $G_s(r, t)$ from $G_0(r, t)$ is maximum, which is achieved when the non-Gaussian parameter[5,6]

$$\alpha_2(t) \equiv \frac{3}{5}\langle r^4(t)\rangle/\langle r^2(t)\rangle^2 - 1 \tag{4}$$

reaches its maximum.

In Figure 2, we see that $G_s(r, t^*)$ and $G_0(r, t^*)$ intersect for large r at r^*, and that $G_s(r, t^*)$ develops a tail for large r falling outside the Gaussian distribution. Molecules with displacements $r > r^*$ can be considered as molecules that move more than expected (in comparison to $G_0(r, t^*)$). We find r^* is in the range 0.20−0.25 nm for all T (the oxygen−hydrogen distance in a molecule for SPC/E is 0.1 nm). The fraction of molecules with $r > r^*$ at $t = t^*$ is given by $\phi \equiv \int_{r^*}^{\infty} 4\pi r^2 G_s(r, t^*)\, dr$. Depending on T, we find $6\% < \phi < 8\%$. For simplicity, we fix $\phi = 7\%$ for all T. Similar values of ϕ were found in atomic systems[36,37,44] and in polymer melts.[51]

Following ref 37, we define the mobility of molecule i at a given time t_0 as the maximum displacement of the oxygen atom in the interval $[t_0, t_0 + \Delta t]$

$$\mu_i(t_0, \Delta t) = \max\{|\vec{r}_i(t_0) - \vec{r}_i(t + t_0)|, t_0 \leq t \leq t_0 + \Delta t\} \tag{5}$$

We will be interested in the "mobile" molecules, defined as the fraction ϕ of molecules with largest μ_i. We define now a connected cluster for an observation time Δt formed by mobile molecules. A pair of molecules is assumed to be connected if

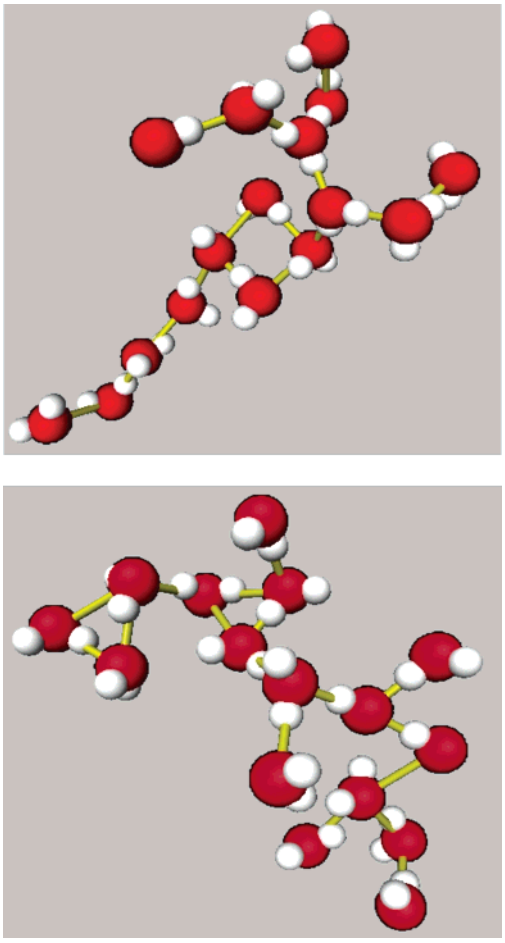

Figure 3. Two of the largest clusters of mobile molecules found at $T = 260$ K defined with an observation time $\Delta t = t^* \approx 3$ ps. Tubes connect neighboring molecules whose oxygen−oxygen distance is less than 0.315 nm, the first minimum in the oxygen−oxygen radial distribution function.

their oxygen−oxygen distance at time t_0 is less than 0.315 nm, which corresponds to the first minimum of the oxygen−oxygen radial distribution function.[71] We find in water that mobile molecule clusters are similar to those in models of simpler liquids. Figure 3 shows two snapshots of mobile particle clusters at $T = 260$ K for $\Delta t = t^*$. In LJ systems[36] and polymers,[52,53] complex clusters are composed of more elementary "strings" in which particles are arranged in a roughly linear fashion. Such linear building blocks of the clusters are less clear in simulations of water because the hydrogen bond network constrains the geometry of the clusters.

A. Dependence of Cluster Size on *t* and Δ*t*. We first address the issue of the dependence of mobile molecule clusters on the observation time Δt. The quantities we study are average cluster size, $\langle n(\Delta t)\rangle$, and the weight average cluster size

$$\langle n(\Delta t)\rangle_w \equiv \frac{\langle n^2(\Delta t)\rangle}{\langle n(\Delta t)\rangle} \tag{6}$$

defined as the average size of a cluster to which a randomly chosen molecule belongs. It is known from percolation theory[54] that clusters of randomly chosen molecules have nontrivial dependence of their sizes on the fraction of chosen molecules, ϕ. To define how the cooperativity affects the cluster sizes, we use a normalized quantity, $\langle n(\Delta t)\rangle_w/\langle n_r\rangle_w$, where $\langle n_r\rangle_w$ is the weight average cluster size for randomly chosen ϕN molecules. Figure 4b shows $\langle n(\Delta t)\rangle$ and $\langle n(\Delta t)\rangle_w$ for $T = 210$ K.

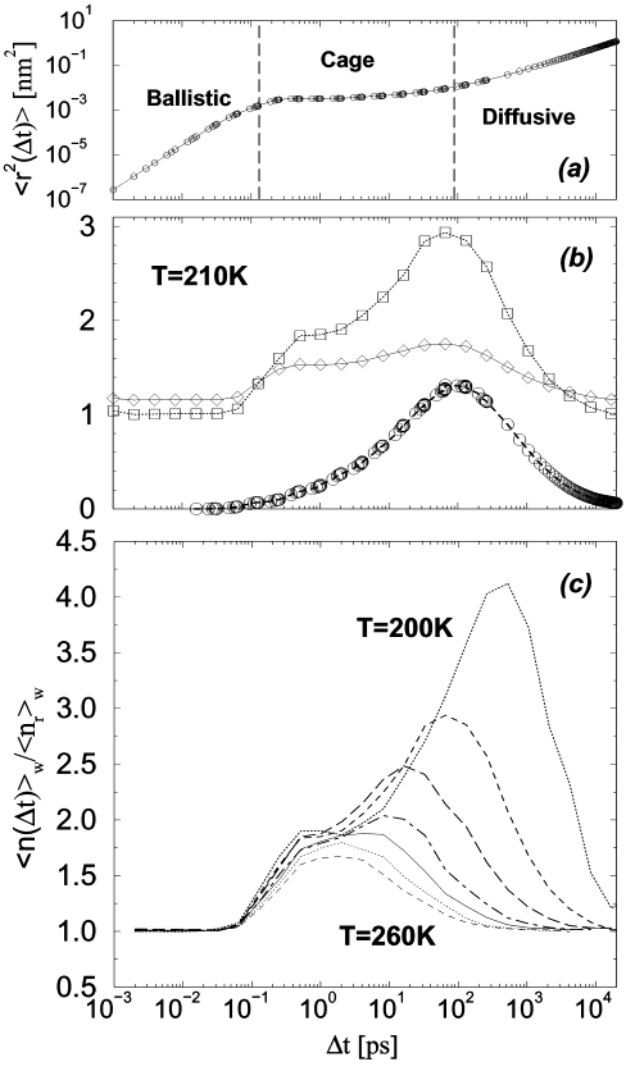

Figure 4. (a) Mean square displacement $\langle r^2(\Delta t)\rangle$ at $T = 210$ K showing the ballistic, cage, and diffusive regimes. (b) Average number of molecules $\langle n(\Delta t)\rangle$ (◇) and normalized weight cluster size $\langle n(\Delta t)\rangle_w/\langle n_r\rangle_w$ (□). The behavior of these quantities correlates with $\langle r^2(\Delta t)\rangle$. The maxima of $\langle n(\Delta t)\rangle_w/\langle n_r\rangle_w$ and $\langle n(\Delta t)\rangle$ occur at times slightly smaller than the time for the maximum in $\alpha_2(\Delta t)$ (○), the non-Gaussian parameter. (c) Weight average cluster size $\langle n(\Delta t)\rangle_w/\langle n_r\rangle_w$ for temperatures ranging from 200 to 260 K in intervals of 10 K. Note the *T*-independent plateau at the crossover from ballistic motion to cage behavior.

For comparison, we show in Figure 4b the non-Gaussian parameter $\alpha_2(\Delta t)$ and the mean-square displacement $\langle r^2(\Delta t)\rangle$ in Figure 4a. The three characteristic time regimes—ballistic, cage, and diffusive—are indicated.

We find that $\langle n(\Delta t)\rangle_w/\langle n_r\rangle_w$ behaves in a way similar to polymer systems[51] but differs in that there is a clear increase in $\langle n(\Delta t)\rangle_w/\langle n_r\rangle_w$ at the time scale at which molecules go from the ballistic to the caged regime. We attribute this to strong correlations in the vibrational motion of the first-neighbor molecules, owing to the presence of hydrogen bonds.

In Figure 4c, we show $\langle n(\Delta t)\rangle_w/\langle n_r\rangle_w$ for all considered *T*. For $T \leq 240$ K, the maximum in $\langle n(\Delta t)\rangle_w/\langle n_r\rangle_w$ increases in magnitude and shifts to larger time scales with decreasing *T*. The plateau at the crossover from the ballistic regime is nearly *T*-independent, as expected since the mean collision time is nearly *T*-independent. For $T \geq 250$ K, the maximum and the plateau merge, so it is not possible to separately distinguish these features.

In the SHD scenario, clusters of mobile molecules appear and disappear continually in time. In Figure 5, we show the

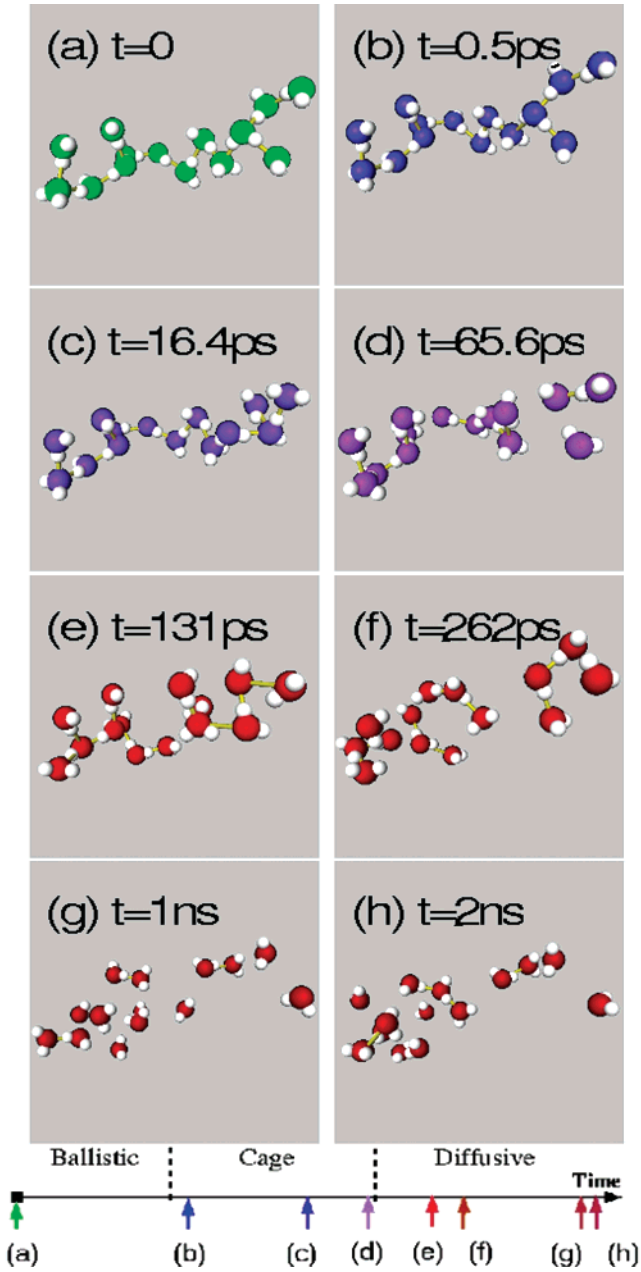

Figure 5. Time evolution of a cluster of mobile molecules identified with $\Delta t = t^* \approx 65$ ps at $T = 210$ K. Time increases from left-to-right and top-to-bottom and is indicated along the time axis (log-scale) at the bottom of the figure. The three regimes (ballistic, cage, and diffusive) defined in Figure 4a are also indicated along the time axis.

time evolution of a cluster defined using $\Delta t = t^* \approx 65$ ps, at $T = 210$ K. We set $t_0 = 0$ as the time at which the cluster is defined. The corresponding snapshot is shown in panel (a). It shows the molecules that will have the largest displacements during the time interval $[t_0, t_0 + \Delta t]$. Their positions at the end of this interval are shown in panel (d). The times of each snapshot are indicated schematically by arrows at the bottom of the figure. Times separating the three regimes (ballistic, cage, and diffusive) are also identified. During the ballistic regime and until the beginning of the cage regime, we observe no change in the cluster structure. During the cage regime, the collisions of the molecules with the neighboring molecules produce little effect. At $t \approx 16.4$ ps, only one molecule of the cluster (at the right end) changes hydrogen bonds. These cumulative small effects produce a split of the cluster as time reaches the end of the cage regime.[72] At $t = t^*$, the cluster splits

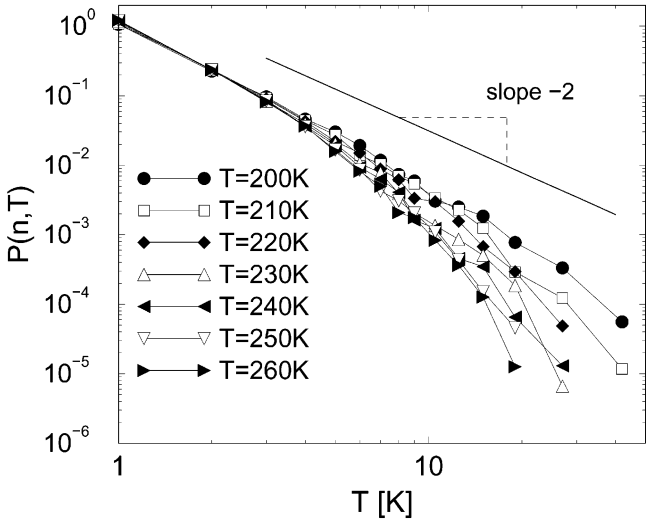

Figure 6. Probability distribution $P(n, T)$ to find a cluster with n molecules at temperature T. Data can be well fitted by $P(n, T) \sim n^{-\tau(T)} \exp(-n/n_0(T))$, eq 7. Values of the parameters $n_0(T)$ and $\tau(T)$ are in Table 1.

TABLE 1: Fitting Parameters for $P(n, T) \sim n^{-\tau(T)} \exp(-n/n_0(T))$, Equation 7

T	$\tau(T)$	$n_0(T)$	T	$\tau(T)$	$n_0(T)$	T	$\tau(T)$	$n_0(T)$
200	2.17	33.4	230	1.96	4.3	250	2.01	4.1
210	1.99	7.4	240	2.04	4.9	260	1.96	3.6
220	2.09	8.0						

into several subclusters. This shows that the cluster no longer behaves as a single entity, and its members possess a certain degree of independence from each other. As expected, for longer times molecules diffuse farther and farther away from each other, and no memory of the starting structure of the cluster remains. During this process, other clusters also appear and disappear in the system.

B. Dependence of Cluster Size on Temperature. We focus now on the temperature dependence of the clusters obtained for $\Delta t = t^*$. Because we use the same definition of clusters as in ref 37, we can compare our results with those found there for a LJ mixture. Figure 6 shows the probability distribution $P(n, T)$ to find a cluster with n molecules for different temperatures T using a fraction $\phi = 0.07$. We note that for this fraction there are no percolating clusters for this system size.

We fit the cluster mass distributions with the *Ansatz* defined in percolation theory[54]

$$P(n, T) \sim n^{-\tau(T)} \exp\left[\frac{-n}{n_0(T)}\right] \qquad (7)$$

where $n_0(T)$ is a characteristic cluster mass (number of molecules) at T and $\tau(T)$ is the Fisher exponent, which may also depend on T. A similar expression for $P(n, T)$ was found in ref 51 for a polymer melt. The parameters in this expression are tabulated in Table 1. Changing the value of ϕ does not affect the functional dependence of $P(n, T)$ although it changes the values of $n_0(T)$ and $\tau(T)$. The values of $n_0(T)$ do not follow a simple dependence on T. However, the behavior of $n_0(T)$ indicates that clusters grow upon cooling. From Table 1, $\tau(T) \approx 2$ for all T. This value coincides with the value obtained for LJ particles $[\tau(T) \approx 1.9]$[37] and for colloids $[\tau(T) \approx 2.2 \pm 0.2]$.[44]

Clusters found in water seem to be smaller than those found in LJ systems. In ref 37, it was found that $P(n, T)$ for $T = 1.07$ T_{MCT} and $\phi = 0.05$ is nonzero up to $n \approx 80$, whereas from Figure 6, we see that even at $T = 200$ K (i.e., 1.03 T_{MCT}) there

are no clusters containing more than 50 molecules. However, the system studied in ref 37 contains 4 times more molecules than our system. This may explain the difference in the cluster size distribution.

III. Spatially Heterogeneous Dynamics and the Cooperatively Rearranging Regions of the AG Theory

The concept of spatially heterogeneous dynamics has a rich history, dating back to the seminal work of Adam and Gibbs[30] (and even AG credit earlier work[55]). Specifically, to describe the dynamics of supercooled liquids,[30,56,57] AG introduced a concept of "cooperatively rearranging regions" (CRR) to describe the diffusion in a low-temperature liquid. Assuming that the heat capacity depends on the inverse temperature, their theory predicts the empirical Williams−Landel−Ferry or Vogel−Fulcher−Tamman equation which determines the evolution of the relaxation time with temperature. Another important result is the relation between the diffusion constant D, the temperature T, and the configurational entropy of the system S_{conf}

$$D \propto \exp\left(\frac{-A}{TS_{conf}}\right) \tag{8}$$

In recent years, S_{conf} has been interpreted, in the thermodynamic limit, as $k_B \log W_c$, where W_c is the number of configurations accessible to the system and k_B is the Boltzmann constant. More recently, W_c has been identified as the number of basins in the PEL accessible to the system in equilibrium, and this allows direct calculation of S_{conf} by computer simulations.[58,59]

Equation 8 has been tested and appears to be valid across a wide spectrum of liquids.[31,32,34,60,61] However, it is based on a somewhat imprecise definition of CRR. In their work, AG define a CRR as "...a subsystem of the sample which, upon a sufficient fluctuation in energy (or, more correctly, enthalpy), can rearrange into another configuration independently of its environment." There is no quantitative definition of CRR. AG predict that the characteristic mass z of the CRR is related to the configurational entropy of the CRR $s_{conf}(z)$ and the total configurational entropy S_{conf} by

$$z = \frac{Ns_{conf}(z)}{S_{conf}} \tag{9}$$

where N is the number of molecules in the liquid.

On the basis of eq 9, we will develop a quantitative definition of CRR in the context of the SHD analysis described in the section above. Motivated by the recent results that the average instantaneous cluster mass scales inversely with the entropy in a model of living polymers[62] and on the basis of eq 9, we use $n^* \equiv \langle n(\Delta t = t^*)\rangle$ as a measure of z, since at $\Delta t = t^*$ correlations are very pronounced and $\langle n(\Delta t)\rangle$ is nearly maximal.[73] Using the values of S_{conf} from ref 31, we find a linear relationship between n^* and $1/S_{conf}$ (Figure 7a)

$$n^* - 1 \propto \frac{1}{S_{conf}} \tag{10}$$

This finding is consistent with the possibility that $n^* - 1$ can be regarded as a measure of z and provides a quantitative connection between mobile molecule clusters and the AG approach.[74] It is necessary to subtract one from n^* to obtain direct proportionality, suggesting that a cluster of unit size does not correspond to a CRR.[37] Equation 10 provides a clear link between a cluster property, n^*, and a property of the PEL, S_{conf}.

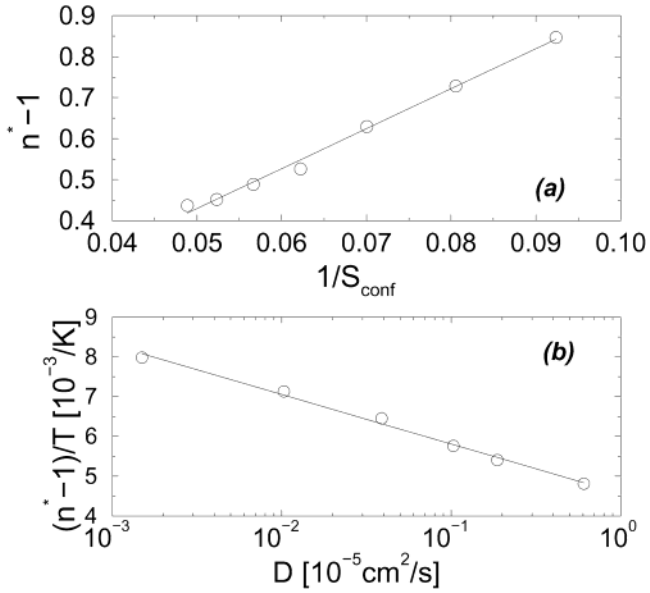

Figure 7. (a) Average cluster size n^* proportional to the inverse of the configurational entropy S_{conf} suggesting that $n^* - 1$ can be used as a measure of the size of the cooperatively rearranging regions hypothesized by Adam and Gibbs. (b) log-linear plot of $(n^* - 1)/T$ as a function of the diffusion constant D. The AG prediction $D \sim \exp(A/TS_{conf})$ implies that $\log D \sim (n^* - 1)/T$. This relationship holds for almost three decades in D.

Since S_{conf} and the diffusion constant D are related,[31] we expect to find

$$D \sim e^{-A(n^*-1)/T} \tag{11}$$

Indeed, Figure 7b confirms this expectation.

IV. Transitions between Inherent Structures

It has been suggested[2,24] that diffusion in low-temperature liquids is a consequence of a more subtle kind of heterogeneity. In principle, these heterogeneities occur when the system moves between consecutive local minima (IS) in the PEL. In this section, we show that clusters of molecules with large displacements when the system moves between consecutive IS can be identified from simulations of water.

As Stillinger suggests,[2,24,25] the PEL is expected to be very rough and contiguous basins are expected to be grouped together forming wider "craters" or "megabasins".[63−65] In this picture, the elementary transition processes (identified with the short-time β-relaxation) connect neighboring basins and require only local rearrangements of a small number of particles. The escape from one large-scale "crater" to another requires a lengthy directed sequence of elementary IS transitions. The process of escape will require a net "elevation change" (energy change) many times that of an elementary IS transition.

The trajectory of the point representing the system on its PEL for any continuous interaction potential can be followed with molecular dynamics simulation, and an energy minimization algorithm can be implemented to find the IS.[23] By means of this method, the motion in configurational space is converted into a minimum-to-minimum trajectory, or IS trajectory. We studied the IS trajectory for a 216-molecule system at $T = 180$ K (below $T_{MCT} \approx 193$ K) using the SPC/E potential.[35] The possibility of performing such a study below T_{MCT}, with a very fine coarse graining in time, allows us to examine the structural changes that accompany the basin transitions and to describe an elementary step of the diffusive process.

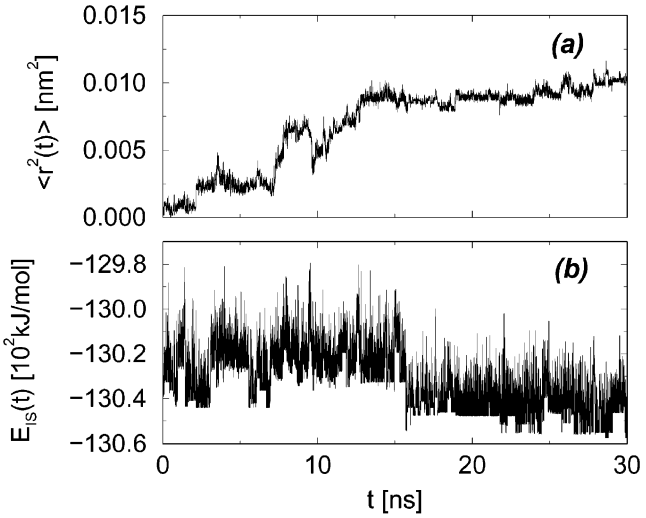

Figure 8. (a) Mean square displacement starting from a single arbitrary starting time and (b) energy of the inherent structures as a function of time for the studied 216-molecule system. The sampling interval in both panels is 1 ps. Although it is possible to track IS transitions from the potential energy, it is not the case for the mean square displacement. Note the amplitude of the peaks of the potential energy is ≈20 kJ/mol, the same order of magnitude as the hydrogen bond energy.

We started our system from equilibrated configurations at 190 K, which relax for nearly 920 ns at 180 K before we record and analyze the trajectory. At such a low temperature, a slow aging in the trajectory could be present; however, the aging should not affect the qualitative picture we present. We generated one trajectory of 30 ns, sampling configurations at each 1 ps. For each configuration, we find the corresponding IS using conjugate gradient minimization. In this way, we obtain 30 000 configurations and the corresponding IS. Since we could miss some IS transitions with 1 ps sampling, we also ran four independent 20 ps simulations sampling the IS at 4 fs. In this way, we obtain another 20 000 configurations with the corresponding IS.

Figure 8 shows an example of the potential energy of the IS trajectory, $E_{IS}(t)$, and the mean square displacement of the oxygen atoms $\langle r^2(t)\rangle$ starting from a single arbitrary starting time. At $T = 180$ K, the slowest collective relaxation time $\tau_\alpha > 200$ ns.[8,9] The IS trajectory in Figure 8 has a mesh of 1 ps and covers a total time of 30 ns. In this time interval, $[\langle r^2(t)\rangle]^{1/2}$ is about 1 Å, i.e., much less than the corresponding value of the average nearest neighbor distance of 2.8 Å. Figure 9 shows an enlargement of the IS trajectory using a much smaller time mesh (4 fs, two times the simulation time step at this T). Figure 9 shows that changes occur via discrete transitions, with an average duration of ≈0.2 ps. The transitions are characterized by an energy change of ≈10−20 kJ/mol and an oxygen atom square displacement of the order of 0.01 Å^2; they appear to constitute the elementary step underlying the diffusional process in the system. Note that it is impossible to identify the transition unless the quenching time step is of the order of the simulation time step, in distinct contrast to a Lennard-Jones liquid where such small continuous changes are not present.[26] The difference, we will see, is attributable to the hydrogen bonds. This time scale for IS transitions agrees with other work on the TIPS2 water model, at $T = 298$ K.[47]

In Figure 9, we see that the sharp changes in $E_{IS}(t)$ coincide with the sharp changes in $\langle r^2(t)\rangle$. This confirms that the system is repeatedly visiting specific configurations, since $\langle r^2(t)\rangle$ and $E_{IS}(t)$ can take only discrete values, corresponding to individual IS. The results shown in Figure 9 imply that the system often returns to the original basin because the differences in energy and the displacement both approach zero at the end of the time interval.

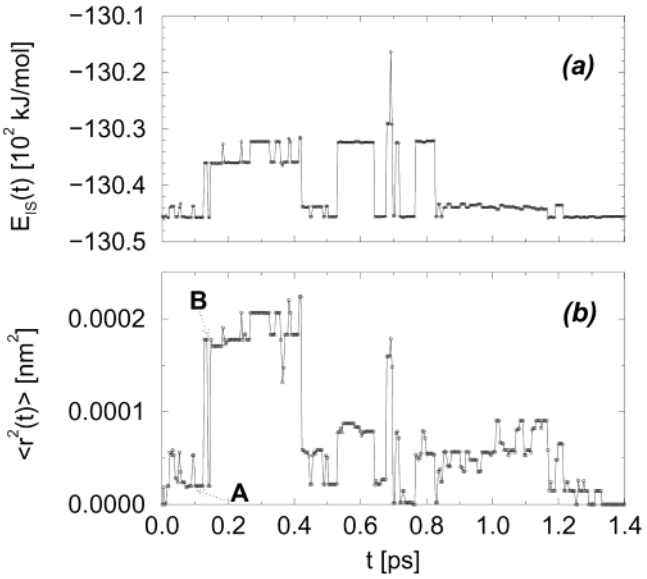

Figure 9. (a) IS energy and (b) mean square displacement for the IS obtained using a sampling interval of 4 fs, two times the simulation time step used at $T = 180$ K. The correlation between E_{IS} and $\langle r^2(t)\rangle$ is evident. Also, we see that it is necessary to sample IS with a mesh of the order of the simulation time step to detect all of the IS visited by the system.

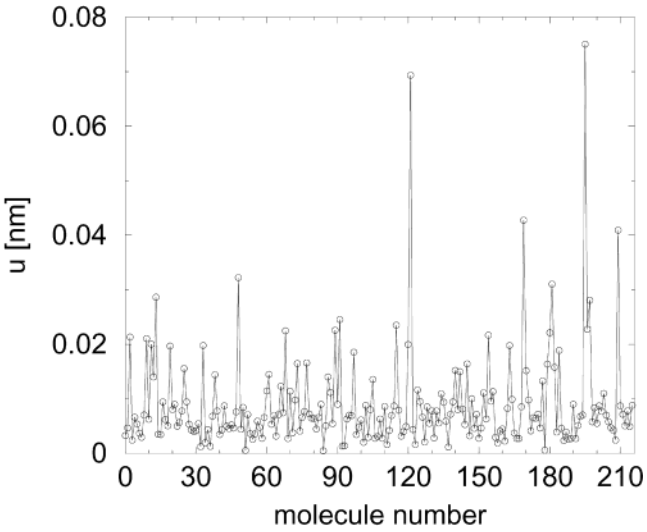

Figure 10. Displacement of each molecule in the transition from IS-A to IS-B shown in Figure 9b.

To aid in understanding the distribution of the displacements during the IS changes such as those between the two IS labeled IS-A and IS−B in Figure 9b, Figure 10 shows the displacements u of all 216 individual molecules from IS-A to IS−B. We see that there is a relatively small set of molecules with a large displacement. Interestingly, we find that this set of molecules forms a cluster of bonded molecules. Indeed, for all cases studied, we find that the set of molecules which displace most ($u \geq 0.025$ nm) form a cluster of bonded molecules. As was shown in ref 35, although a subset of "highly mobile" molecules is identifiable using a pre-defined threshold value in a single basin change, there is no unambiguous general criterion for identifying the molecules responsible for a single basin transition.

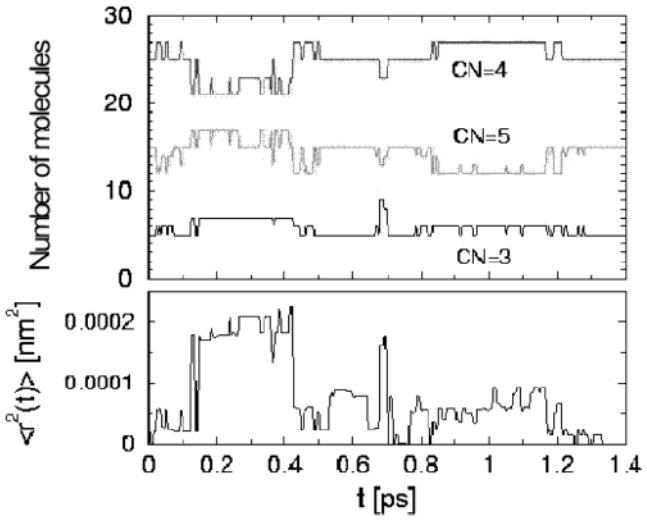

Figure 11. Number of molecules with coordination number (CN) of 3−5 versus time, for the IS corresponding to Figure 9. The plot for CN = 4 is shifted down by 196 units for better comparison. The bottom panel shows $\langle r^2(t)\rangle$. We see how the tetrahedral network acquires both types of defects (CN equals to 3 and 5) while the system explores different IS.

Water is characterized by a tetrahedral hydrogen bond (HB) network. However, many experiments suggest that this network has defects, such as an extra (fifth) molecule in the first coordination shell.[66−70] The clusters identified in the IS transition are related to the re-structuring of the HB network, as can be observed in Figure 11 where we show the number of molecules with a coordination number equal to 3 (low-density defect), 4, or 5 (high-density defect) as functions of time for a characteristic time interval and contrast these data with the time dependence of $\langle r^2(t)\rangle$. A clear anticorrelation is observed between the time dependence of the number of 3-coordinated and 5-coordinated molecules compared to the time dependence of the 4-coordinated molecules. The changes in the numbers of HB are connected with jumps in $\langle r^2(t)\rangle$, indicating that the HB changes occur when the system changes IS.[35]

V. Discussion

We have shown that SHD is present in MD simulations of water. In accordance with experiments in colloids and simulations of simple liquids, the mobile molecule clusters grow in size as T decreases. To connect with AG theory, we have shown that the average mass of these clusters can be interpreted as the mass of the AG cooperatively rearranging regions. By studying the PEL, we have shown that molecules with large displacements in IS transitions also form clusters. Preliminary calculations show that clusters obtained in IS transitions and those obtained in the original MD trajectory are uncorrelated.

Acknowledgment. We thank F. Sciortino and S. G. Glotzer for enlightening discussions. This work was supported by NSF Chemistry Grant CHE 0096892.

References and Notes

(1) Angell, C. A. *Science* **1995**, *267*, 1924.
(2) Debenedetti, P. G.; Stillinger, F. H. *Nature (London)* **2001**, *410*, 259.
(3) Glotzer, S. C. *J. Non-Cryst. Solids* **2000**, *274*, 342.
(4) Ediger, M. D.; Angell, C. A.; Nagel, S. R. *J. Phys. Chem.* **1996**, *100*, 13200.
(5) Sciortino, F.; Gallo, P.; Tartaglia, P.; Chen, S. H. *Phys. Rev. E* **1996**, *54*, 6331.
(6) Sciortino, F.; Fabbian, L.; Chen, S.-H.; Tartaglia, P. *Phys. Rev. E* **1997**, *56*, 5397.
(7) Kob, W.; Anderson, H. C. *Phys. Rev. Lett.* **1994**, *73*, 1376.
(8) Starr, F. W.; Sciortino, F.; Stanley, H. E. *Phys. Rev. E* **1999**, *60*, 6757.
(9) Harrington, S.; Sciortino, F.; Stanley, H. E. *Phys. Rev. Lett.* **1999**, *82*, 3629.
(10) Schmidt-Rohr, K.; Spiess, H. W. *Phys. Rev. Lett.* **1991**, *66*, 3020.
(11) Liesen, J.; Schmidt-Rohr, K.; Spiess, H. W. *J. Non-Cryst. Solids* **1994**, *172−174*, 737.
(12) Heuer, A.; Wilhelm, M.; Zimmermann, H.; Spiess, H. W. *Phys. Rev. Lett.* **1995**, *75*, 2851.
(13) Cicerone, M. T.; Ediger, M. D. *J. Chem. Phys.* **1995**, *103*, 5684.
(14) Fujara, F.; Geil, B.; Sillescu, H.; Fleischer, G. *Z. Phys. B* **1992**, *88*, 195.
(15) Cicerone, M. T.; Blackburn, F. R.; Ediger, M. D. *J. Chem. Phys.* **1995**, *102*, 471.
(16) Hurley, M.; Harrowell, P. *Phys. Rev. E* **1995**, *52*, 1694.
(17) Mel'cuk, A. I.; Ramos, R. A.; Gould, H.; Klein, W.; Mountain, R. D. *Phys. Rev. Lett.* **1995**, *75*, 2522.
(18) Muranaka, T.; Hiwatari, Y. *Phys. Rev. E* **1995**, *51*, R2735.
(19) Kob, W.; Donati, C.; Plimpton, S. J.; Poole, P. H.; Glotzer, S. C. *Phys. Rev. Lett.* **1997**, *79*, 2827.
(20) Poole, P. H.; Glotzer, S. C.; Coniglio, A.; Jan, N. *Phys. Rev. Lett.* **1997**, *78*, 3394.
(21) Angell, C. A.; Ngai, K. L.; McKenna, G. B.; McMillan, P. F.; Martin, S. W. *J. Appl. Phys.* **2000**, *88*, 3113.
(22) Goldstein, M. *J. Chem. Phys.* **1969**, *51*, 3278.
(23) Stillinger, F. H.; Weber, T. A. *Phys. Rev. A* **1983**, *28*, 2408.
(24) Stillinger, F. H. *Science* **1995**, *267*, 1935.
(25) Sastry, S.; Debenedetti, P. G.; Stillinger, F. H. *Nature (London)* **1998**, *393*, 554.
(26) Schrøder, T. B.; Sastry, S.; Dyre, J. C.; C Glotzer, S. *J. Chem. Phys.* **2000**, *112*, 9834.
(27) Heuer, A. *Phys. Rev. Lett.* **1997**, *78*, 4051. Buchner, S.; Heuer, A. *Phys. Rev. E* **1999**, *60*, 6507.
(28) Angelani, L.; Parisi, G.; Ruocco, G.; Villani, G. *Phys. Rev. Lett.* **1998**, *81*, 4648.
(29) Sciortino, F.; Kob, W.; Tartaglia, P. *Phys. Rev. Lett.* **1999**, *83*, 3214.
(30) Adam, G.; Gibbs, J. H. *J. Chem. Phys.* **1965**, *43*, 139.
(31) Scala, A.; Starr, F. W.; La Nave, E.; Sciortino, F.; Stanley, H. E. *Nature (London)* **2000**, *406*, 166.
(32) Sastry, S. *Nature (London)* **2001**, *409*, 164.
(33) Speedy, R. *J. Phys. Chem. B* **1999**, *103*, 4060.
(34) Speedy, R. *J. Chem. Phys.* **2001**, *114*, 9069.
(35) Giovambattista, N.; Starr, F. W.; Sciortino, F.; Buldyrev, S. V.; Stanley, H. E. *Phys. Rev. E* **2002**, *65*, 041502.
(36) Donati, C.; Douglas, J. F.; Kob, W.; Plimpton, S. J.; Poole, P. H.; Glotzer, S. C. *Phys. Rev. Lett.* **1998**, *80*, 2338.
(37) Glotzer, S. C.; Poole, P. H.; Kob, W.; Plimpton, S. J. *Phys. Rev. E* **1999**, *60*, 3107.
(38) Doliwa, B.; Heuer, A. *Phys. Rev. Lett.* **1998**, *80*, 4915.
(39) Böhmer, R.; et al. *Europhys. Lett.* **1996**, *36*, 55.
(40) Schiener, B.; et al. *Science* **1996**, *274*, 752.
(41) Kegel, W. K.; van Blaaderen, A. *Science* **2000**, *287*, 290.
(42) Sillescu, H. *J. Non-Cryst. Solids* **1999**, *243*, 81.
(43) Ediger, M. D. *Annu. Rev. Phys. Chem.* **2000**, *51*, 99.
(44) Weeks, E. R.; et al. *Science* **2000**, *287*, 627.
(45) Berendsen, H. J.; et al. *J. Phys. Chem.* **1987**, *91*, 6269.
(46) Sciortino, F.; Geiger, A.; Stanley, H. E. *Nature* **1991**, *354*, 218.
(47) Ohmine, I.; Tanaka, H. *Chem. Rev.* **1993**, *93*, 2545 and references therein.
(48) Götze, W. *J. Phys.: Condens. Matter* **1999**, *11*, A1.
(49) Götze, W. In *Liquids, Freezing and Glass Transition*; Hansen, J. P., Levesque, D., Zinn-Justin, J., Eds.; North-Holland, Amsterdam, 1991.
(50) Hansen, J. P.; McDonald, I. R. *Theory of Simple Liquids*; Academic Press: London, 1986.
(51) Gebremichael, Y.; Schrøder, T. B.; Starr, F. W.; Glotzer, S. C. *Phys. Rev. E* **2001**, *64*, 051503.
(52) Bennemann, C.; Baschnagel, J.; Glotzer, S. C. *Nature* **1999**, *399*, 246.
(53) Aichele, M.; Gebremichael, Y.; Starr, F. W.; Baschnagel, J.; Glotzer, S. C. *J. Chem. Phys.* **2003**, *119*, 5290.
(54) Stauffer, D.; Aharony, A. *Introduction to Percolation Theory*; Taylor and Francis: London, 1998.
(55) Jenckel, E. *Z. Phys. Chem.* **1939**, *184*, 309.
(56) Debenedetti, P. G. *Metastable Liquids*; Princeton University Press: Princeton, 1996.
(57) Debenedetti, P. G. *J. Phys.: Condens. Matter* **2003**, *15*, 1669.
(58) Stillinger, F. H.; Weber, T. A. *J. Phys. Chem.* **1983**, *87*, 2833.

(59) Coluzzi, B.; Parisi, G.; Verrocchio, P. *Phys. Rev. Lett.* **1999**, *84*, 306.
(60) Mossa, S.; et al. *Phys. Rev. E* **2002**, *65*, 041205.
(61) Speedy, R. *J. Phys. Chem. B* **2001**, *105*, 11737.
(62) Dudowicz, J.; Freed, K. F.; Douglas, J. F. *J. Chem. Phys.* **1999**, *111*, 7116.
(63) Doliwa, B.; Heuer, A. *Phys. Rev. E* **2003**, *67*, 030501.
(64) Doliwa, B.; Heuer, A. *Phys. Rev. E* **2003**, *67*, 031506.
(65) Denny, R. A.; Reichman, D. R.; Bouchaud, J.-P. *Phys. Rev. Lett.* **2003**, *90*, 025503.
(66) *Hydrogen Bonded Liquids*; Dore, J., Texeira, J., Eds.; Kluwer: Dordrecht, The Netherlands, 1991; pp 171−183.
(67) Grunwald, E. *J. Am. Chem. Soc.* **1986**, *108*, 5719.
(68) Narten, A. H.; Levy, H. A. *Science* **1969**, *165*, 447.
(69) Giguere, P. A. *J. Chem. Phys.* **1987**, *87*, 4835.
(70) Walrafen, G. E.; Hokmabadi, M. S.; Yang, W. H.; Chu, Y. C.; Monosmith, B. *J. Phys. Chem.* **1989**, *93*, 2909.
(71) Alternatively, we also consider using a separation of 0.35 nm, the distance criterion commonly used by hydrogen bond definitions [Sciortino, F.; Fornili, S. L. *J. Chem. Phys.* **1989**, *90*, 2786]. Preliminary calculations indicated this alternative choice does not qualitatively affect our results.
(72) For our particular case, at the beginning of the diffusive regime, molecules are able to recombine forming two residual subclusters.
(73) The maximum of $\langle n(\Delta t)\rangle$ occurs at time slightly before t^*. Our conclusions are unaffected by choosing n^* or the maximum of $\langle n(\Delta t)\rangle$.
(74) This connection relies on the assumption that the T dependence of $s_{conf}(z)$ is weak in comparison to that of S_{conf}, as can be expected since $z \ll N$ and the configurational entropy is an extensive property.